phenomenon was also observed for a MB with a fluorophore/quencher design. While having not been reported previously, this observation can be understood considering that the distance between donor and acceptor when MB is in the open form (usually 20–30 mer in length) is not significantly larger than the Förster distance (around 65 Å in this case). Thus there is considerable FRET between the donor and acceptor for MBs in the open form. This process is also manifested by the appearance of a fluorescence spectrum of MB in the open form (Figure 2b), where the FAM emission is still significant. The design of the MB with two fluorophores also provides an easy and effective way of measuring the Förster energy transfer distance for a given donor/acceptor pair. The efficiency of energy transfer can be calculated from the quenching of the donor emission in the presence of the acceptor. By designing two-fluorophore MBs with different lengths (number of bases as shown in MB1 and MB3 in Table 1), Förster energy transfer distance for a given donor/acceptor pair can thus be determined using the FRET efficiency with these different MBs.

In conclusion, we have proposed a new strategy of designing MBs which uses two fluorophores instead of one fluorophore and one quencher as the donor and acceptor. Such MBs display high sensitivity and a large dynamic range. Molecular beacons of this new design with coumarin and 6-FAM as the fluorophores can quantitatively detect the target DNA up to 1×10^{-7} M with a detection limit of 1.7×10^{-10} M with a basic spectrometer. It could also be very useful for studying protein–DNA/RNA interactions,[8] where the fluorophores are as likely to be pulled apart as to be squeezed closer. We were also able to determine for the first time the Förster distance for the coumarin/FAM pair, which was estimated to be 65 ± 1 Å. We expect MBs of this design to be effective for applications in both DNA/RNA and protein–DNA/RNA interaction studies as well as in genetic analysis based on better linearity, larger dynamic range, higher sensitivity, and less dependence on optical geometry and photobleaching.

Received: June 13, 2000
Revised: October 4, 2000 [Z15249]

[1] S. Tyagi, F. R. Kramer, *Nat. Biotechnol*. **1996**, *14*, 303–308.
[2] S. Tyagi, D. Bratu, F. R. Kramer, *Nat. Biotechnol*. **1998**, *16*, 49–53; A. S. Piatek, S. Tyagi, A. C. Pol, A. Telenti, L. P. Miller, F. R. Kramer, D. Alland, *Nat. Biotechnol.* **1998**, *16*, 359–363.
[3] D. L. Sokol, X. Zhang, P. Lu, A. M. Gewirtz, *Proc. Natl. Acad. Sci. USA* **1998**, *95*, 11538–11543; X. Fang, J. Li, J. Perlette, K. Wang, W. Tan, *Anal. Chem.* **2000**, *72*, 747A–753A.
[4] X. Fang, X. Liu, S. Schuster, W. Tan, *J. Am. Chem. Soc.* **1999**, *121*, 2921–2922; X. Liu, W. Tan, *Anal. Chem.* **1999**, *71*, 5054–5059.
[5] W. Chen, G. Martinez, A. Mulchandani, *Anal. Biochem*. **2000**, *280*, 166–172.
[6] J. J. Li, R. Geyer, W. Tan, *Nucleic Acids Res.* **2000**, e52, *28*, 1–5.
[7] L. G. Kostrikis, S. Tyagi, M. M. Mhlanga, D. D. Ho, F. R. Kramer, *Science* **1998**, *279*, 1228–1229.
[8] L. G. Kostrikis, Y. X. Huang, J. P. Moore, S. M. Wolinsky, L. Q. Zhang, Y. Guo, L. Deutsch, J. Phair, A. U. Neumann, D. D. Ho, *Nat. Med.* **1998**, *4*, 350–353.
[9] J. J. Li, X. Fang, S. M. Schuster, W. Tan, *Angew. Chem.* **2000**, *112*, 1091–1094; *Angew. Chem. Int. Ed.* **2000**, *39*, 1049–1052; X. Fang, J. Li, W. Tan, *Anal. Chem*. **2000**, *72*, 3250–3258.
[10] J. R. Lakowicz, *Principles of Fluorescence Spectroscopy*, 2nd ed., Kluwer, New York, **1999**.
[11] M. Yang, M. E. McGovern, M. Thompson, *Anal. Chim. Acta* **1997**, *346*, 259–275.
[12] A. H. Uddin, P. A. E. Piunno, R. H. E. Hudson, M. J. Damha, U. J. Krull, *Nucleic Acids Res.* **1997**, *25*, 4139–4146.

An Exceptionally Stable Ti Superoxide Radical Ion: A Novel Heterogeneous Catalyst for the Direct Conversion of Aromatic Primary Amines to Nitro Compounds**

Gajanan K. Dewkar, Milind D. Nikalje, Iliyas Sayyed Ali, Abhimanyu S. Paraskar, H. S. Jagtap, and A. Sudalai*

Superoxide ion ($O_2^{\bullet -}$), an active oxygen species, plays important roles in various diseases caused by oxygen toxicity such as ischemia, carcinogenesis, inflammation, diabetes, and aging.[1] Superoxide dismutases act as a defense system against oxygen toxicity in living cells by catalyzing the dismutation of $O_2^{\bullet -}$ into H_2O_2 and O_2.[2] Although it is normally reduced to H_2O, O_2 may diffuse out of the electron-transport enzyme system and interact with important biological molecules.[3] In spite of much research, neither the mode nor the site of damage due to $O_2^{\bullet -}$ in biological systems is known. Investigations on the organic chemistry of $O_2^{\bullet -}$ with simple model substances have shown that $O_2^{\bullet -}$ is a versatile species[4] and can behave as a base, as a nucleophile, and as an oxidizing or reducing agent,[5] but none of this provides an explanation for its toxicity. While the debate regarding the importance of $O_2^{\bullet -}$ in vivo continues, the chemistry of the radical remains to be completely characterized. Consequently, it is of interest to study the reactions of $O_2^{\bullet -}$ with simple organic molecules such as amines to build up a picture of its possible biological effects.

A literature search[2a, 4], [6] reveals that the generation of $O_2^{\bullet -}$ is achieved by electrolytic reduction of O_2 in DMF or by enzymes such as xanthine-xanthine oxidase. Recently, the generation of $O_2^{\bullet -}$ was described on the lattice of metal oxides such as MgO/CaO, ZnO, ZrO_2, and TiO_2 by using a photo-induced electron-transfer process.[7] However, these methods

[*] Dr. A. Sudalai, G. K. Dewkar, M. D. Nikalje, I. Sayyed Ali, A. S. Paraskar, H. S. Jagtap
Process Development Division
National Chemical Laboratory
Pune 411008 (India)
Fax: (+91) 20-5893359
E-mail: sudalai@dalton.ncl.res.in

[**] The authors are thankful to Dr. Devotta and the Director, NCL for their constant encouragement. Three of us (G.K.D., M.D.N., and I.S.A.) also thank CSIR for the award of an Senior Research Fellowship (SRF). Suggestions from the referees are highly appreciated.

Supporting information for this article is available from the author.

are not suitable for large-scale synthesis. Here we report a new and practical method for the generation of $O_2^{\bullet-}$ on a solid hydrated titanium matrix and its catalytic activity towards N–H bonds of aromatic and aliphatic primary amines.

The light yellow Ti superoxide catalyst **1** was prepared by the action of 50% H_2O_2 on $Ti(OR)_4$ in anhydrous MeOH at 25 °C [Eq. (1)]. It was characterized by FTIR, ESR, and Raman spectroscopy, X-ray diffraction (XRD), thermogravimetric/differential thermal analysis (TG/DTA), and elemental analysis. Its IR spectrum shows characteristic absorption bands at 3720 (w), 3665 (w), and 3450 cm^{-1} (s) that indicate the presence of vibrational modes of coordinated water molecules on a Ti^{4+} site and of surface TiOH groups.[8] The other IR absorption bands at 1027 (s) and 1157 cm^{-1} (m) indicate the presence of superoxide radical ion on the solid material.[7b, 9] It also has IR bands in the range of 900–538 cm^{-1} (m) corresponding to the presence of Ti-O-Ti linkages. An intense line at 900 cm^{-1} in the Raman spectrum of the catalyst further confirmed the presence of Ti-O-Ti linkages. The other weak Raman lines observed in the range of 1025–1119 cm^{-1} were assigned to $O_2^{\bullet-}$.

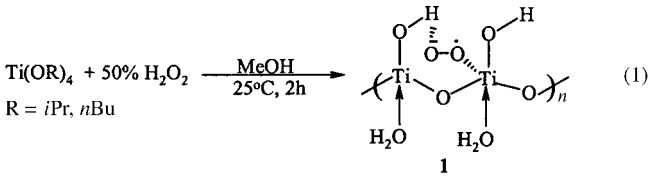

(1)

The XRD pattern of **1** shows that it is amorphous, as there are no sharp peaks in the spectrum. A sample of **1** dried at 25 °C (3 mm Hg) shows characteristic ESR signals at $g_1 = 2.024$, $g_2 = 2.009$, and $g_3 = 2.003$ (Figure 1), which strongly

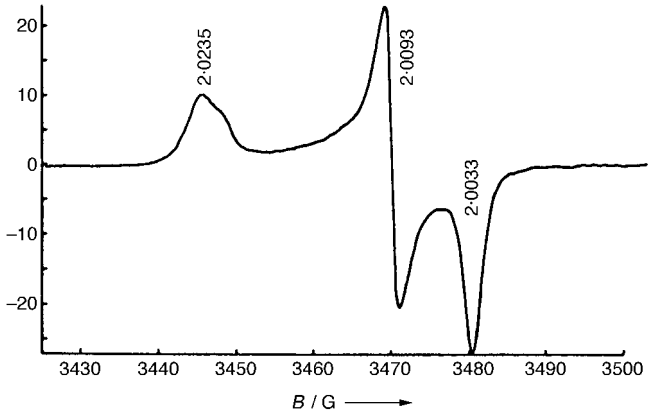

Figure 1. ESR spectrum of **1** at 298 K.

suggest the presence of unpaired electrons of the stable superoxide radical anion generated by the decomposition of H_2O_2 on the Ti matrix.[7c,f, 10] However, when **1** was dried at 90 °C (3 mm Hg), the characteristic ESR signals were absent, that is, the superoxide radical anions are lost at higher temperature.

The TG/DTA analysis of **1** (Figure 2) shows a weight loss of 22.59% at 114 °C and of 10.84% at 291 °C due to the loss of coordinated H_2O molecules and superoxide radical anion, respectively. Volumetric analysis[11] of **1** gave Ti content of 41.7%, and the surface area, determined by the Brunauer–Emmett–Teller method, was 310 $m^2 g^{-1}$.

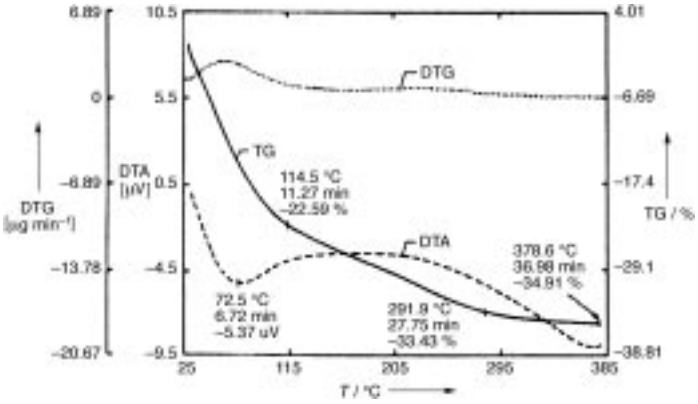

Figure 2. TG/DTA spectrum of **1**.

To evaluate the catalytic activity of **1**, various primary amines were subjected to oxidation with 50% H_2O_2 at 25 °C (Table 1). In the case of aromatic amines, the reaction selectively afforded the corresponding nitro derivatives in high yields. This result is particularly interesting because oxidation of amines is generally complicated by several other competing reaction pathways that yield a range of products.[12] Product selectivity depends on the H_2O_2/amine molar ratio, and at higher ratios (H_2O_2/amine = 6/1) the selectivity for nitro derivatives is high. Remarkably, even arylamines with electron-withdrawing groups such as COOH and NO_2 are efficiently oxidized to the corresponding nitroarenes (entries 11 and 12), which otherwise may be difficult to obtain by conventional nitration methods. The high selectivity for nitrobenzenes may be rationalized by the high Ti content (41.7%) of the solid catalyst.

Under similar oxidation conditions, aliphatic primary amines with α-CH bonds are selectively converted to oximes along with the ketone formed by partial hydrolysis thereof. It can be reasoned that the α-CH protons of species **C** (see Scheme 2) undergo prototropic migration to give a more stable enol form. It is also possible that attack of nitroso species **C** on the electrophilic oxygen atom of the peroxide associated with the Ti matrix is preferred due to the higher basicity of the nitroso compound compared to its oxime counterpart (Scheme 1).

To obtain more information on the nature of the reactive intermediate in the oxidation of amines, the following experiments were carried out: 1) The oxidation of aniline with 50% H_2O_2 and **1** as catalyst was monitored by ESR spectroscopy. When the catalyst **1** was added to a solution of aniline in methanol, the characteristic ESR signal of the catalyst disappeared. However, the ESR signal reappeared on the addition of a small

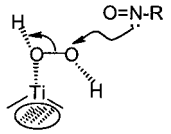

Scheme 1. Attack of nitroso species on the electrophilic oxygen atom of the peroxide associated with the Ti matrix.

  1433-7851/01/4002-0406 $ 17.50+.50/0 *Angew. Chem. Int. Ed.* **2001**, *40*, No. 2

Table 1. Oxidation of amines with **1** as catalyst.[a]

$ArNH_2 \xrightarrow[25\,^\circ C,\ 0.5\,h]{\mathbf{1},\ H_2O_2,\ MeOH} ArNO_2$

Entry	Substrate	Time [min]	Conversion [%]	Product[b] selectivities [%][c]			
				NB	NSOB	AB	AZOB
Aromatic amines							
1	aniline	30	100	98.18	1.82	–	–
2	2-methylaniline	30	100	97.35	1.50	–	1.15
3	3-methylaniline	35	100	90.00	6.60	1.50	1.90
4	4-methylaniline	30	100	98.00	1.57	–	0.43
5	2-methoxyaniline	30	100	97.15	1.00	0.80	1.05
6	2-methoxy-5-nitroaniline	35	100	95.60	3.05	–	1.35
7	4-methoxyaniline	30	100	97.05	1.13	0.37	1.45
8	4-hydroxyaniline	45	100	89.22	3.01	3.62	4.15
9	2-methyl-6-ethylaniline	35	100	90.98	4.50	1.87	2.65
10	4-chloroaniline	35	100	91.22	5.00	1.50	2.28
11	4-nitroaniline	45	100	82.50	9.01	3.19	5.31
12	2-aminobenzoic acid	45	100	85.05	8.05	4.09	2.81
Aliphatic amines					Oxime		Ketone
1	cyclohexyl amime	45	90		88.88		11.11
2	benzylamine	45	85		94.11		5.88
3	ethylenediamine	45	80		87.5		12.5

[a] Catalyst was recovered and reused without any loss of activity and selectivity. [b] Products were characterized by m.p., IR, ^{1}H NMR, MS, and GC-MS. [c] Selectivities are based on gas chromatographic analysis; NB = nitrobenzene, NSOB = nitrosobenzene, AB = azobenzene, AZOB = azoxybenzene.

quantity of 50 % H_2O_2. As the reaction progressed, this signal again became weak and finally disappeared. 2) The oxidation of primary amines did not take place when a radical quencher was added to the reaction mixture. To explain these results, the catalytic cycle shown in Scheme 2 is proposed.

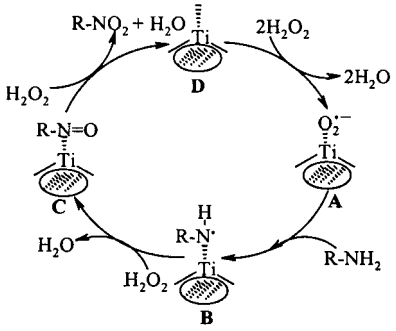

Scheme 2. Proposed catalytic cycle for the oxidation of amines.

The first step is the abstraction of a hydrogen atom from the amine by the superoxide radical anion **A** to generate the transient RNH$^\bullet$ radical **B**,[13] which is oxidized by H_2O_2 to nitroso species **C**. Further oxidation of **C** with 1 mol of H_2O_2 generates nitrobenzene and liberates **D**. Finally the superoxide catalyst **A** is regenerated by decomposition of hydrogen peroxide on the Ti^{4+} surface [Eqs. (2) and (3)].[7f,g, 14]

$$Ti^{4+} + H_2O_2 \longrightarrow 2\,{}^\bullet OH \quad (2)$$

$$^\bullet OH + H_2O_2 \longrightarrow H_2O + O_2^{\bullet -} + H^+ \quad (3)$$

To determine whether the catalyst behaves in a truly heterogeneous manner, it was filtered off at the end of the reaction, and an additional amount of aniline and H_2O_2 was added to the reaction mixture. No nitrobenzene was obtained, and aniline was completely recovered. Further, the catalyst recovered by simple filtration was successfully reused for the oxidation of aniline.

In conclusion, we have demonstrated a novel method for the preparation of a stable Ti superoxide catalyst **1** from readily and cheaply available Ti(O*i*Pr)$_4$. Catalyst **1** is heterogeneous and very effective for the selective oxidation of amines, particularly of anilines and aliphatic primary amines, to the corresponding nitrobenzenes and oximes. We are currently investigating the use of this novel material for other oxidations such as epoxidation and dihydroxylation of olefins, sulfoxidation, and hydroxylation of phenol.

Experimental Section

1: 50 % H_2O_2 (5.98 g, 0.175 mol) was added slowly to a solution of Ti(O*i*Pr)$_4$ (5.0 g, 0.0175 mol) in anhydrous MeOH (50 mL) over 40 min under N_2 with stirring at room temperature. The yellow precipitate that formed was collected by filtration on a sintered funnel, washed with anhydrous methanol, and dried under reduced pressure (3 mm Hg) at 25 °C for 1 h. Yield: 3.94 g (98 %). EPR spectra were recorded on a Bruker EMX spectrometer at 9.76 GHz and 298 K, and g values were determined relative to a standard marker: α,α'-diphenyl-β-picryl hydrazyl (DPPH, g = 2.0036). TG/DTA was performed on a TG/DTA 22, TG/DTA 32 system (Seiko Instruments) in the range of 30 – 400 °C at 10 °C min$^-$.

Oxidation of aniline: 50 % aqueous H_2O_2 (2.19 g, 0.064 mol) was added slowly to a mixture of aniline (1.0 g, 0.011 mol), **1** (0.25 g, 25 wt %), and anhydrous methanol (15 mL) under N_2 with stirring over 10 min. The reaction was exothermic, and the color changed from yellow to reddish brown during addition of H_2O_2. The reaction was monitored by TLC (15 % ethyl acetate in petroleum ether (60 – 80 °C)) and after completion, catalyst **1** was filtered off, and methanol evaporated under reduced pressure. The crude product (1.3 g) was analyzed by gas chromatography.

Received: January 3, 2000
Revised: October 16, 2000 [Z 14492]

[1] W. Ando, *Organic Peroxides*, Wiley, Chichester, **1992**, p. 729.
[2] a) A. Meister, *Adv. Enzymol. Relat. Areas Mol. Biol.* **1974**, *41*, 39; b) G. Crank, M. I. H. Makin, *Aust. J. Chem.* **1984**, *37*, 2331; c) A. G. Sykes, *Adv. Inorg. Chem.* **1998**, *45*, 127.
[3] D. J. Stuehr, M. A. Marletta, *J. Org. Chem.* **1985**, *50*, 694.

  1433-7851/01/4002-0407 $ 17.50+.50/0

[4] a) E. Lee-Ruff, *Chem. Soc. Rev.* **1977**, *6*, 195; b) A. A. Frimer, G. Aljadeff, J. Ziv, *Chem. Soc. Rev.* **1983**, *48*, 1700.
[5] a) D. T. Sawyer, J. S. Valentine, *Acc. Chem. Res.* **1981**, *14*, 393; b) G. E. Davico, V. M. Bierbaum, *J. Am. Chem. Soc.* **2000**, *122*, 1740; c) A. A. Viggiano, S. T. Arnold, R. A. Morris, A. F. Ahrens, P. M. Hierl, *J. Phys. Chem.* **1996**, *100*, 14397; d) W. H. Koppnol, *Nature* **1976**, *262*, 420.
[6] A. A. Frimer in *The Chemistry of Peroxides* (Ed.: S. Patai), Wiley, **1983**, p. 429.
[7] a) R. Kokes, *Proc. Int. Congr. Catal. 3rd*, *1964* (Amsterdam, 20–25 July), **1965**, p. 484; b) J. Ragai, *Nature* **1987**, *325*, 703; c) A. Amorelli, J. C. Evans, C. C. Rowlands, *Chem. Soc. Faraday Trans. 1*, **1988**, *84*, 1723; d) P. Tengvall, L. Bertilsson, B. Liedberg, H. Elwing, I. Lundstrom, *J. Colloid Interface Sci.* **1990**, *139*, 575; e) A. Tuel, J. Diab, P. Gelin, M. Dufuax, J.-F. Dutel, Y. B. Taarit, *J. Mol. Catal.* **1990**, *63*, 95; f) M. Anpo, M. Che, B. Fubini, E. Garrrone, E. Giamello, M. C. Paganini, *Top. Catal.* **1999**, *8*, 189; g) E. Giamello, L. Calosso, B. Fubini, F. Geobaldo, *J. Phys. Chem.* **1993**, *97*, 5735.
[8] J. L. G. Fierro, *Stud. Surf. Sci. Catal.* **1990**, *57A*, 196.
[9] I. Q. Long, H. L. Wan, *J. Chem. Soc. Faraday Trans. 2* **1997**, *93*, 355.
[10] M. Shiotani, G. Moro, J. H. Freed, *J. Chem. Phys.* **1981**, *74*, 2616.
[11] a) *Standard Methods of Chemical Analysis*, *Vol. 1* (Ed.: N. H. Furman), D. V. Nostral, Princeton, NJ, **1962**; b) M. Mori, M. Shibata, E. Kyuno, S. Ito, *Bull. Chem. Soc. Jpn.* **1956**, *29*, 904.
[12] a) G. Crank, M. I. H. Makin, *Aust. J. Chem.* **1984**, *37*, 845; b) H. R. Sonawane, A. V. Pol, P. P. Moghe, S. S. Biswas, A. Sudalai, *J. Chem. Soc. Chem. Commun.* **1994**, 1215; c) S. Gontier, A. Tuel, *Appl. Catal. A* **1994**, *118*, 173; d) T. Selvam, A. V. Ramaswamy, *Catal. Lett.* **1995**, *31*, 103; e) S. Gontier, A. Tuel, *J. Catal.* **1995**, *157*, 124; f) S. Suresh, R. Joseph, B. Jayachandran, A. V. Pol, M. P. Vinod, A. Sudalai, H. R. Sonawane, T. Ravidranthan, *Tetrahedron* **1995**, *51*, 11305; g) M. Besson, M. C. Bonnet, P. Gallezof, I. Tkatchenko, A. Tuel, *Catal. Today* **1999**, *51*, 547.
[13] F. Haber, J. Weiss, *Proc. R. Soc. London A* **1934**, *147*, 332.
[14] a) W. Koppenol, J. Butler, *FEBS Lett.* **1977**, *83*, 1; b) I. Kazarnovskii, A. B. Neiding, *Dokl. Akad. Nauk. SSSR* **1952**, *86*, 717.

Parallel Synthesis of ZSM-5 Zeolite Films from Clear Organic-Free Solutions**

Re Lai, Beom Seok Kang, and George R. Gavalas*

High-throughput synthesis and screening ("combinatorial") techniques have been recently introduced to the discovery and optimization of solid-state materials,[1–3] such as phosphors,[4] superconductors,[5] dielectrics,[6] and heterogeneous catalysts.[7–11] In this study parallel synthesis is applied to prepare supported ZSM-5 zeolite films. Identifying compositions that produce a microscopically continuous zeolite film usually constitutes the first step in zeolite membrane synthesis,[12, 13] an area that has attracted considerable attention in the last decade due to prospective gas separation applications.[13–17] Zeolite films are also of interest for sensor and nonlinear optical material applications.[18, 19] Zeolite film synthesis, in which film thickness, composition, and even crystallite orientation can be controlled,[19–22] offers an interesting approach to the preparation of catalytic libraries.

There are several reports on the parallel synthesis of zeolite powders.[23–25] Akporiaye and co-workers developed a convenient multiwell autoclave wherein one hundred or more distinct reaction mixtures could be treated hydrothermally. The solid products were washed in situ and transferred to individual sample holders for X-ray analysis.[23] Other groups employed post-synthetic treatment to attach the powder products to a silicon wafer or filter paper to eliminate the need for individual sample handling. X-ray microdiffraction was then used to identify individual sample members. Klein et al.[24] used a silicon wafer as the bottom of a multiwell autoclave and, after reaction, heated the precipitates to bond them to the wafer. They also applied this technique to produce zeolite libraries for catalytic investigation.[26] Bein and coworkers designed a centrifuge apparatus that allowed quantitative product recovery onto filter paper without manipulation of individual samples.[25]

Parallel film synthesis in the present study was carried out in a multiwell reactor similar to that used in reference [24]. The reactor, shown schematically in Figure 1, contains twenty-one wells of approximately 3 mm diameter and 5 mm depth

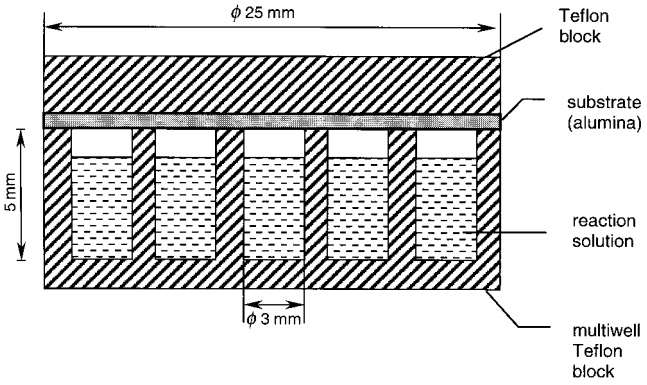

Figure 1. Cross-section of the multiwell reactor.

drilled in a Teflon block. After the solutions had been introduced, the substrate alumina disk was placed on top of the wells and was covered by a cylindrical Teflon block. The sandwich was enclosed in a Parr reaction bomb, with the Teflon cap of the bomb applying the necessary pressure for sealing the wells. No additional water was added into the bomb. The diameter of the substrate disk was 2.5 cm, chosen to fit in the sample holder of the scanning electron microscope (SEM). The volume of solution in each well was 35 μL, a little less than the 40 μL volume of the wells. To ensure full contact of the substrate with the solution, the bomb was inverted and gently shaken several times with the substrate at the bottom of the solution and then placed in the oven either with the substrate placed horizontally at the bottom of the synthesis solution, or was rotated by 90° to fix the substrate in a vertical position. Upon opening the autoclave at the completion of the reaction no loss of liquid from the wells was observed and all zeolite films were found firmly attached to the substrate. The morphology of the films was examined by scanning electron

[*] Prof. G. R. Gavalas, R. Lai, Dr. B. S. Kang
Division of Chemistry and Chemical Engineering
California Institute of Technology
Pasadena, CA 91125-4100 (USA)
Fax: (+1) 626-568-8743
E-mail: gavalas@cheme.caltech.edu

[**] This study was funded by the Chevron Research and Technology Co.

  1433-7851/01/4002-0408 $ 17.50+.50/0